

Bulged-out nucleotides protect an antisense RNA from RNase III cleavage

Tord Å. H. Hjalte and E. Gerhart H. Wagner*

Department of Microbiology, Biomedical Center, Uppsala University, Box 581, S-751 23 Uppsala, Sweden

Received December 5, 1994; Revised and Accepted January 9, 1995

ABSTRACT

Bulged-out nucleotides or internal loops are present in the stem-loop structures of several antisense RNAs. We have used the antisense/target RNA system (CopA/CopT) that controls the copy number of plasmid R1 to examine the possible biological function of bulged-out nucleotides. Two regions within the major stem-loop of the antisense RNA, CopA, carry bulged-out nucleotides. Base pairing in either one or both of these regions of the stem was restored by site-specific mutagenesis and in one case a new internal loop was introduced. The set of mutant and wild-type CopA variants was characterized structurally *in vitro*. The results reported here indicate a possible function of the bulges: their presence protects CopA RNA from being a substrate for the double-strand-specific enzyme RNase III. *In vitro* cleavage rates were drastically increased when either the lower or both bulges were absent. This is paralleled by a similar, but not identical, effect of the bulges on metabolic stability of the CopA RNAs *in vivo*. The degradation pathways of wild-type and mutant CopA in various strain backgrounds are discussed. In the accompanying paper, we address the significance of bulges in CopA for binding to the target RNA *in vitro* and for its inhibitory efficiency *in vivo*.

INTRODUCTION

Antisense RNAs are key regulators of a variety of biological activities in, primarily, prokaryotic accessory elements like phages, plasmids and transposons (1). They act as efficient inhibitors of functions of target RNAs. The inhibition is post-transcriptional and involves antisense/target RNA base pairing. Two main parameters affect the efficiency of antisense RNA control, the rate constants for the binding between antisense and target RNA and the intracellular concentration of the inhibitor. Mutations in the DNA encoding the complementary RNAs generally decrease binding rate constants (2,3), whereas antisense RNA concentrations are most easily affected by mutations in genes encoding enzymes involved in RNA turnover (4,5).

Naturally occurring antisense RNAs in prokaryotes are usually small, untranslated and highly structured. Most of these RNAs have been shown to consist of stem-loop structures, often connected by single-stranded regions or flanked by single-stranded tails. Extensive research has been carried out on

plasmids R1 and ColE1, where antisense RNAs control plasmid copy number, and on transposon *Tn10*, where translation of transposase mRNA is inhibited by an antisense RNA (reviewed in 1). In R1, an antisense RNA (CopA) is the main copy number control element (6). CopA is constitutively transcribed and turned over rapidly *in vivo*. This implies that the intracellular concentration of CopA RNA represents a measure of the copy number of the plasmid (for a recent review, see 7). CopA, by binding to its target, the leader region of the RepA mRNA (CopT), inhibits the synthesis of the initiator protein, RepA. This inhibition is indirect and involves translational coupling between a leader peptide reading frame (*tap*) and *repA* (8,9).

The relationship of structure and function of antisense RNAs is a topic of interest, since features that govern performance of the inhibitor RNA are amenable to study and lessons learned from the well-defined systems may guide the design of efficient artificial antisense RNAs. We used the CopA/CopT system of plasmid R1 to study the contribution of structural properties to the efficiency of antisense RNA control; similar approaches have been reported for other systems (for example 10,11). Previous studies showed that nucleotides in loop regions are involved in primary recognition. For plasmid R1, this conclusion was supported by the copy number phenotypes of naturally occurring point mutants as well as those created by site-specific mutagenesis (6,9,12). An optimal loop size of the recognition loop II (Fig. 1) for high binding rates was shown to be 5-7 (12). For complete antisense/target RNA pairing, a single-stranded region has to be present (13).

Most antisense RNAs identified so far carry bulged-out nucleotides or internal loops within stem regions, close to the recognition loops. Is the presence of these interruptions within helical domains of importance for the effectiveness of the antisense RNA? Destabilization of helical domains can affect the metabolic stability of the RNA, since exonuclease activity is dependent on the ΔG^0 of such structures (see, for example, 14) and cleavage by RNase III is affected by the degree of double-strandedness (15). If the metabolic stability is altered, steady-state levels of the antisense RNAs change and thus inhibitory activity is altered accordingly. Since two regions within the upper CopA stem II display such bulges, we asked whether restored base pairing within this region would affect one or other of the two most important parameters for inhibition: binding rates and metabolic stability. We introduced mutational changes into *copA* so that one or both of the bulges in CopA were removed or, in addition, a new internal loop was introduced. The local effects of the mutations on CopA structure were verified by

* To whom correspondence should be addressed

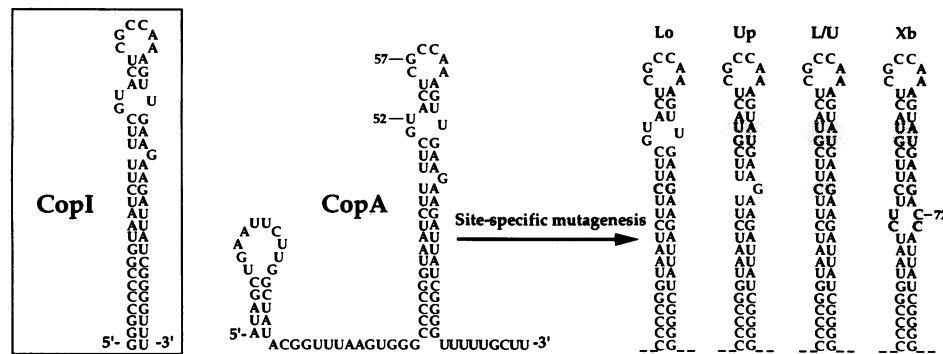


Figure 1. The locations of the mutational changes in CopA used in this study. The secondary structure of CopA is shown (23). Changes introduced into stem-loop II are indicated by shaded boxes. The wild-type, truncated CopA species (CopI) used in some of the experiments is shown to the left. For easier interpretation of cleavage site positions in Figures 3 and 6, some nucleotide positions are indicated (U_{52} and G_{57} in CopA-Wt; C_{72} in CopA-Xb).

chemical and enzymatic probes. Gel mobility assays indicated that bulge removal causes a drastic overall structure change. The effect of the mutations shows that bulges can protect CopA from cleavage by RNase III, both *in vitro* and *in vivo*. Alterations in the degradation pathway for mutant and wild-type CopAs in several different strain backgrounds are discussed.

In the accompanying paper we show that the presence of the bulges is also important for obtaining high binding rates *in vitro* and maximal inhibition of *repA* expression *in vivo* (16).

MATERIALS AND METHODS

Bacterial strains

Bacterial strains used are shown in Table 1. The *Escherichia coli* strain MC1061 was used as host for plasmid constructions and NM522 for the production of single-stranded (+) DNA from the pGW58 plasmids for site-specific mutagenesis (12). For Northern analyses we used four strains. The parental strain, IBPC5321, is wild-type with respect to the *mc* and the *pcnB* loci respectively. Mutant alleles were introduced by P1 transduction; the *mc14::Tn10* allele by using lysates from strain HT115 (Rnc null phenotype) into IBPC5321, selecting for tetracycline resistance; the *pcnB* mutation with lysates from MM38K (17), selecting for kanamycin resistance (a gene encoding kanamycin resistance is inserted between the deletion end points).

Plasmid constructions

Plasmids used in this study are shown in Table 1. Plasmid pGW58 (18) was described previously and served as the parent for the plasmids carrying the mutant *copA* genes. The mutagenesis protocol used to introduce the bulge mutations into *copA* has been described previously (12,19,20). Mutagenic oligodeoxyribonucleotides are listed below.

In the plasmids of the pGW58-CA series (see Northern analyses, Fig. 7; Table 3) the *repA* promoter was deleted, so that CopA RNA could be analyzed without CopT transcription. The pGW58 plasmids were cut with *EcoRI*, followed by fill-in using the Klenow enzyme and dNTPs. Subsequently, the linearized plasmids were partially cut with *XmnI*. The 4.2 kb *XmnI*-*EcoRI* (blunt) fragment containing the R1 control region (deleted for the *repA*

promoter) was isolated, self-ligated and digested with *AseI* to destroy self-ligated, full-length plasmid DNA that had failed to be cleaved by *XmnI*. The 4.2 kb fragment was re-isolated, self-ligated and transformed into MC1061 cells.

To construct plasmids for *in vitro* transcription of CopI RNAs, pUC19 DNA was cleaved with *EcoRI* and *HindIII*. Four phosphorylated oligodeoxyribonucleotides were annealed, pairwise (T7-up and T7-down; SLII-up and SLII-down), to give double-stranded fragments for insertion into the cleaved pUC19 vector DNA. The T7-up/down fragment had an *EcoRI* overhang preceding a T7 promoter sequence and a downstream blunt end, and the SLII-up/down fragment a blunt end followed by the sequence of the wild-type stem-loop II, some additional base pairs and a *HindIII* overhang. A *DraI* site was appropriately generated for cleavage and subsequent *in vitro* run-off transcription. An *Apal* site present at the start of the stem-loop II sequence facilitates introduction of mutant *copA* sequences. Plasmids pGW16-Up, pGW16-Lo, pGW16-L/U and pGW16-Xb were derived from pGW-16 by insertion of double-stranded oligodeoxyribonucleotides carrying the mutant stem-loop II sequences into pGW16.

Oligodeoxyribonucleotides

Oligodeoxyribonucleotides were synthesized on an Applied Biosystems 394 DNA/RNA Synthesizer. Mutagenic oligodeoxyribonucleotides for site-specific mutagenesis of *copA* were: 5'-GGT AAT CTT CTT CGT ACT CGC C (TH-Lo); 5'-CGC CAA AGT ATG AAG AAG (TH-up); 5'-AGT ATG AAG ACC ATT ATC GGG G (TH-Xb).

For construction of pGW16, the following four oligodeoxyribonucleotides were made: 5'-AAT TCG AAA TTA ATA CGA CTC ACT ATA G (T7-Up); 5'-CTA TAG TGA GTC GTA TTA ATT TCG (T7-down); 5'-GGC CCC GGT AAT CTT TTC GTA CTC GCC AAA GTT GAA GAA GAT TAT CGG GGT TTA AAT GCA GGT A (SLII-up); 5'-AGC TTA CCT GCA TTT AAA CCC CGA TAA TCT TCT TCA ACT TTG GCG AGT ACG AAA AGA TTA CCG GGG CC (SLII-down). For plasmids pGW16-Lo, -Up, -L/U and -Xb, the following pairs were used respectively: 5'-CCG GTA ATC TTC TTC GTA CTC GCC AAA GTT GAA GAA GAT TAT CGG GGT TTA A (TH-Lo1) and 5'-AGC TTT AAA CCC CGA TAA TCT TCT TCA ACT TTG GCG AGT ACG AAG AAG ATT ACC GGG GCC (TH-Lo2); 5'-CCG GTA ATC TTT TCG TAC TCG CCA AAG TAT GAA GAA GAT TAT

CGG GGT TTA A (TH-Up1) and 5'-AGC TTT AAA CCC CGA TAA TCT TCT TCA TAC TTT GGC GAG TAC GAA AAG ATT ACC GGG GCC (TH-Up2); 5'-CCG GTA ATC TTC TTC GTA CTC GCC AAA GTA TGA AGA AGA TTA TCG GGG TTT AA (TH-L/U1) and AGC TTT AAA CCC CGA TAA TCT TCT TCA TAC TTT GGC GAG TAC GAA GAA GAT TAC CGG GGC C (TH-L/U2); 5'-CCG GTA ATC TTC TTC GTA CTC GCC AAA GTA TGA AGA CCA TTA TCG GGG TTT AA (TH-Xb1) and 5'-AGC TTT AAA CCC CGA TAA TGG TCT TCA TAC TTT GGC GAG TAC GAA GAA GAT TAC CGG GGC C (TH-Xb2).

PCR primers were: 5'-GAA ATT AAT ACG ACT CAC TAT AGT AGC TGA ATT GTT GGC TAT ACG (T7-AS); 5'-AAA GCA AAA ACC CCG ATA ATC TTC (T7-AE); 5'-GAA ATT AAT ACG ACT CAC TAT AGG TTA AGG AAT TTT GTG GCT GG (T7-GG); 5'-CGTTT GGTGA AGATC AGTCA CACC (T7T-E1).

As a probe for 5S rRNA (in Fig. 7) we used 5'-TAC GGC GTT TCA CTT CTG AGT TTG GG (GW-5S).

Cell growth and media

Cells were grown in LB medium (21) supplemented with 0.2% glucose. The solid medium, LA, was LB with 1.5% (w/v) agar. When appropriate, ampicillin (50 µg/ml), chloramphenicol (30 µg/ml), kanamycin (50 µg/ml) and tetracycline (15 µg/ml) were included.

Enzymes and chemicals

Enzymes and chemicals were of the highest purity available. Restriction enzymes for cloning procedures were bought from New England Biolabs or Pharmacia. Purified RNase III was a generous gift from D.Court (NCI, Frederick, MD). Radiochemicals were purchased from DuPont NEN.

DNA manipulations

Purification of plasmid DNA, restriction enzyme cleavages and other DNA techniques were essentially according to Sambrook *et al.* (22).

Electrophoretic mobility shifts of CopI RNAs

Plasmids (pGW16 series) were cleaved with *DraI*. Uniformly labelled CopI RNAs were transcribed from the linearized templates by T7 RNA polymerase in the presence of [α -³²P]UTP (12). RNAs were purified from sequencing gels (12). For analysis, aliquots of wild-type and mutant CopI RNAs were run on either 8% sequencing gels at 300 V and 18 mA (semi-denaturing conditions) or at 2000 V and 30 mA (fully denaturing conditions). In both cases, samples were boiled in formamide dye (FD) (13) and placed on ice before loading. Alkaline ladders (from 5'-end-labelled CopT; 23) were run in parallel, in order to assess the relative difference in migration of the CopI species.

Table 1. (A) *Escherichia coli* strains used and (B) plasmids used

A	Strains	Genotype	Source/reference	
	MC 1061	<i>araD139, (Δara-leu)7697, lacZ74, galU, hsdR, rpsL</i>	[35]	
	NM522	<i>supE, thi, hsd5, Δ(lac-proAB), [F', proA⁺B⁺, lacI^qZM 15]</i>	[36]	
	IBPC5321	F ⁻ , <i>thi-1, argG6, argE3, his-4, mtl-1, xyl-5, tsx-29, rpsL, ΔlacX74</i>	[37]	
	IBPC5321- <i>rnc</i> ⁰	as IBPC5321, but <i>rnc14::Tn10</i>	This work	
	IBPC5321- <i>rnc</i> ⁰ - <i>pncB</i> ⁰	as IBPC5321, but <i>rnc14::Tn10</i> and <i>pncB::aah</i>	This work	
	IBPC5321- <i>pncB</i> ⁰	as IBPC5321, but <i>pncB::aah</i>	This work	
B	Plasmids	Description	Parent plasmid(s)	Source/reference
	pGW58	Cloned R1 control region, -296 to +596 ^a	pMa5-8 + pJL133	[18]
	pGW58-Lo	as pGW58, but lower bulge C insertion ^b	pGW58	This work
	pGW58-Up	As pGW58, but upper bulge A insertion ^b	pGW58	This work
	pGW58-L/U	as pGW58, but double mutant ^b	pGW58-Lo	This work
	pGW58-Xb	as pGW58-L/U, but + artificial bulge ^b	pGW58-L/U	This work
	pGW16	CopI transcription template	pUC 19	This work
	pGW16-Lo	CopI transcription template	pGW16	This work
	pGW16-Up	CopI transcription template	pGW16	This work
	pGW16-L/U	CopI transcription template	pGW16	This work
	pGW16-Xb	CopI transcription template	pGW16	This work
	pGW58-CA	Deleted <i>repA</i> promoter, carries <i>copA</i> gene	pGW58	This work
	pGW58-CA-Lo	as pGW58-CA, but <i>copA-Lo</i>	pGW58-Lo	This work
	pGW58-CA-Up	as pGW58-CA, but <i>copA-Up</i>	pGW58-Up	This work
	pGW58-CA-L/U	as pGW58-CA, but <i>copA-L/U</i>	pGW58-L/U	This work
	pGW58-CA-Xb	as pGW58-CA, but <i>copA-Xb</i>	pGW58-Xb	This work

^aNumbers refer to nucleotide positions in (38).

^bReferring to CopA structure (see Fig. 1).

Ribonuclease A probing of CopA RNA

Structural mapping by RNase A was performed on 5'-end-labelled RNA, using the protocol described in Wagner and Nordström (23). On average much less than one cut per molecule was introduced.

Lead(II) acetate probing of CopA RNA

Lead(II) acetate mapping was performed on 5'-labelled RNA essentially according to Gornicki *et al.* (24) and Hardt *et al.* (25). Incubations (volume 10 μ l) contained ~20 000 c.p.m. of CopA in buffer L (20 mM Tris-OAc, pH 7.5, 100 mM NaCl, 118 mM MgCl₂). After pre-incubation (5 min at 37°C), lead(II) acetate was added to 10 mM final concentration. After an additional 5 min, reactions were stopped by 2 μ l of 50 mM Na₂EDTA and 10 μ l FD. Samples were boiled prior to electrophoresis.

Northern blot analysis

Isolation of total cellular RNA and Northern analysis was as described (18). As a CopA probe, a PCR fragment encoding CopT was transcribed in the presence of [α -³²P]UTP [see accompanying paper (16)]. Pre-hybridization of the membranes was done at 65°C for 1 h, hybridization overnight at 42°C with washing twice in 2 \times SSC, 0.5% SDS at 42°C (20 min). Probing for 5S rRNA was performed with the oligodeoxyribonucleotide GW-5S (see above). Band intensities were quantified using a Molecular Dynamics PhosphorImager.

In vitro transcription of CopA and RNAI by *E. coli* RNA polymerase

Supercoiled plasmid DNA preparations of the pGW58 series were transcribed by *E. coli* RNA polymerase (Pharmacia) with [γ -³²P]ATP and unlabelled NTPs (2). Under these conditions the label is preferentially incorporated into CopA RNA and RNAI (both RNAs initiate with ATP). The RNAs were phenol-treated, precipitated (with carrier tRNA) and dissolved in water. An equal volume of FD was added, samples boiled and then loaded on an 8% sequencing gel.

In vitro RNase III cleavage assays

CopA RNAs were synthesized by T7 RNA polymerase transcription from PCR-generated DNA fragments (12). 5'-labelled CopA was generated by removal of the 5'-terminal phosphates (using calf intestinal phosphatase; Pharmacia) and subsequent phosphorylation with [γ -³²P]ATP and T4 polyribonucleotide kinase (Pharmacia). Assays were done in 38 μ l of cleavage buffer (18). 5'-end-labelled pre-tRNA was included so that both RNAs were present at approximately the same c.p.m. and total yeast tRNA (Sigma Chemicals) was included at 50 μ g/ml. After pre-incubation (5 min at 37°C), an 8 μ l aliquot was withdrawn and phenol added (minus enzyme control). Then, 1 μ l of appropriately diluted RNase III (determined in pilot experiments to yield a measurable time course of cleavage) was added to the remaining 30 μ l. After 30 s and 6 and 12 min respectively, 8 μ l aliquots were withdrawn. After phenolization, precipitation and resuspension in water, an equal volume of FD was added. Samples were boiled prior to loading on 8% sequencing gels. Dried gels were analyzed by PhosphorImager analyses. The band intensities of full-length CopA RNA were corrected using the band intensity of the (not cleaved) pre-tRNA

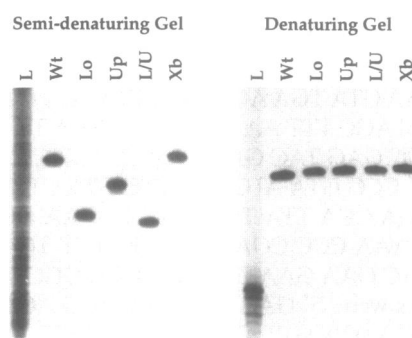


Figure 2. Electrophoretic mobility of mutant CopI species determined by semi-denaturing gel electrophoresis. Uniformly labelled CopI RNAs were applied to 8% sequencing gels and electrophoresed either under semi-denaturing conditions (Materials and Methods) (left autoradiogram) or, as a control, under denaturing conditions to show that the molecular sizes of the CopI RNAs were as expected (right hand panel). Mutant and wild-type CopI species are indicated on top of the Figure. L, alkaline ladder used to assess relative differences in CopI migration.

as a reference. In these assays, RNase III was estimated to be in excess over labelled CopA for all incubations. In accord with this, plots of decrease in the intensity of the CopA band over time yielded essentially first order kinetics. The slopes of these curves were used to calculate relative cleavage rates, by correcting for enzyme concentration.

The salt dependence of RNase III cleavage was assayed in the same way, except that pre-mixtures lacked sodium chloride and aliquots of appropriate NaCl solutions were added prior to incubation to obtain the concentrations shown in Figure 5,

RESULTS

The effects of bulge mutations on overall and local structure of CopA

Wild-type CopA carries two regions in the upper stem of stem-loop II where bulged-out nucleotides are present. Site-directed mutagenesis was used to introduce changes in the *copA* gene, so that the CopA species encoded had the upper (CopA-Up), lower (CopA-Lo) or both bulges (CopA-L/U) removed (see Fig. 1). An additional construction, derived from *copA-L/U*, carries a new internal loop close to the center of stem II (CopA-Xb). CopI RNA of mutant or wild-type origin (consisting of only stem-loop II; see Fig. 1 and Materials and Methods) was transcribed *in vitro* and analyzed on either semi-denaturing or denaturing (sequencing) gels. Figure 2 shows that, in particular, CopA-Lo and CopA-L/U migrate much faster than suggested by their molecular size (cf. their migration on the denaturing gel), indicating that the absence of the bulges drastically alters the structure of the stem-loop. CopA-Up shows a smaller effect and CopA-Xb appears unaffected.

The presence or absence of bulges in CopA RNA can be analyzed by using structure-specific enzymes or chemicals (for a review, see 26). We used RNase A and lead(II) acetate respectively to probe the secondary structures of the *in vitro* transcribed, 5'-end-labelled, purified RNAs in solution. Wild-type and mutant CopAs were partially digested with RNase A or reacted with lead(II) acetate. Autoradiograms of such experiments are shown in

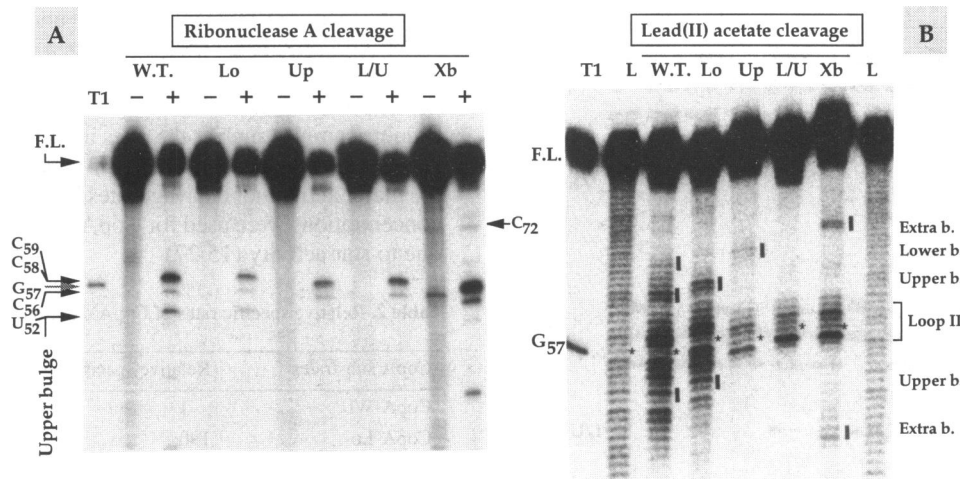


Figure 3. Probing of CopA RNA structure by RNase A and lead(II) acetate. (A) Partial RNase A digestions were carried out on 5'-end-labelled CopA RNA species as described (Materials and Methods; 23). An autoradiogram of such an analysis is shown. The various CopA species used are indicated; (+) or (-) indicates incubations in the presence or absence of RNase A and T1 represents a digest of CopA-Wt with RNase T1 (positional marker, stippled arrow; T1 cleaves the single G₅₇ nucleotide in loop II; see Fig. 1). F.L. shows the position of full-length CopA, cleavages specific for the upper bulge (U₅₂ (23) are indicated and C residues within loop II are shown by solid arrows. For Xb, cleavage at the new internal loop is indicated (C₇₂). (B) 5'-end-labelled CopA RNAs were partially cleaved as described in Materials and Methods. The RNAs were separated on an 8% sequencing gel and an autoradiogram is shown. T1 indicates digestion of CopA-Wt with RNase T1 and L is an alkaline ladder. The mutant and wild-type RNA species are indicated. The positions of G₅₇ (asterisks) and the bulges (solid bars) are indicated.

Figure 3. RNase A is specific for single-stranded pyrimidines and thus cleaves within the upper bulge (23). Figure 3A demonstrates these cleavages and shows the absence of this bulge in CopA-Up and CopA-L/U. The predicted internal loop of CopA-Xb is also apparent (see Figs 1 and 3A).

Lead(II) acetate can be used as a convenient probe to detect, in particular, conformational changes in RNAs (24). The chemical cleaves generally within loops and interhelical regions (bulges and internal loops). We used lead(II) acetate to probe for the presence and absence of the bulges predicted for the mutant and wild-type CopA variants. Figure 3B shows that bulges predicted to be present yield lead cleavage-specific bands. The newly introduced internal loop of CopA-Xb is detected as well. Furthermore, CopA-Wt and CopA-Lo, the two RNAs in which the upper bulge is still present, show increased cleavage extending from the loop region into the upper stem, indicating a higher degree of breathing within the topmost 3 bp of the stem.

Removal of bulges renders CopA sensitive to cleavage by RNase III

RNase III is a ribonuclease that readily cleaves all double-stranded RNAs, apparently without major sequence specificity (15). The minimal length of a double-stranded RNA recognized and cleaved by the enzyme is ~20 bp, equivalent to two helical turns. Removal of bulges within the major CopA stem-loop (~25 bp including three possible G:U base pairs at the bottom end of the stem) might therefore render the RNA susceptible to RNase III cleavage. We tested this possibility by assaying cleavage rates of 5'-end-labelled CopA with purified RNase III. In initial titration experiments, we determined the amount of enzyme needed to yield measurable cleavage on the time scale chosen. RNase III was kept in excess over the RNA, i.e. we were measuring initial rates under conditions where CopA cleavage followed first order kinetics. An internal standard (a 5'-end-labelled pre-tRNA) was included to correct for unequal loading of the gel. This RNA is an extremely poor substrate and stayed unaffected throughout the experiment. Figure

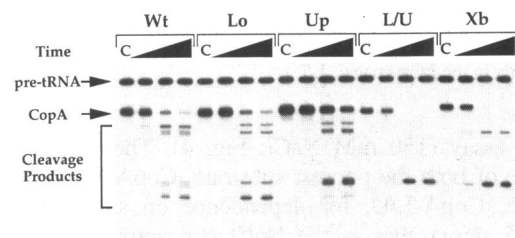


Figure 4. *In vitro* cleavage of CopA RNAs by purified RNase III. Time courses of cleavage were analysed by gel electrophoresis on 8% sequencing gels according to Materials and Methods. Incubations contained, in addition to CopA, a 5'-end-labelled pre-tRNA. Cleavage products are indicated by brackets; for detailed mapping of the cleavage positions see Figure 6. C denotes control incubations in the absence of enzyme. The filled triangles indicate increasing incubation times (30 s and 6 and 12 min). RNase III concentrations used were as follows: 5.7 (CopA-Wt), 0.57 (CopA-Up), 0.057 (CopA-Lo; CopA-Xb) and 0.0057 μ g/ml (CopA-L/U). Quantitations of this experiment (and others) are summarized in Table 2.

4 shows the time courses of cleavage of the different CopA species. Note that the enzyme concentrations used were adjusted to yield measurable rates (see legend to Fig. 4). The specific rates of cleavage were obtained by quantification of the decrease in the bands corresponding to full-length CopA (corrected for loading) divided by the concentration of enzyme used. Decay rates were obtained from the slopes of linear-log diagrams. These results from three experiments like the one in Figure 4 are shown in Table 2. All four mutant CopA species were cleaved at rates higher than that of CopA-Wt. The CopA variant lacking both bulges, CopA-L/U, displayed the highest rate of cleavage.

It is known that RNase III can effectuate secondary site cleavage activity when low salt or very high enzyme concentrations are used (15,27). To obtain measurable cleavage rates *in vitro* with the CopA-Wt substrate, high enzyme concentrations had to be used (Fig. 4). Previous *in vivo* analyses indicated that free CopA was not an RNase III substrate, whereas CopA-CopT RNA duplexes were cleaved rapidly (18). In bacteria, salt concentrations are assumed to be significantly higher than in our

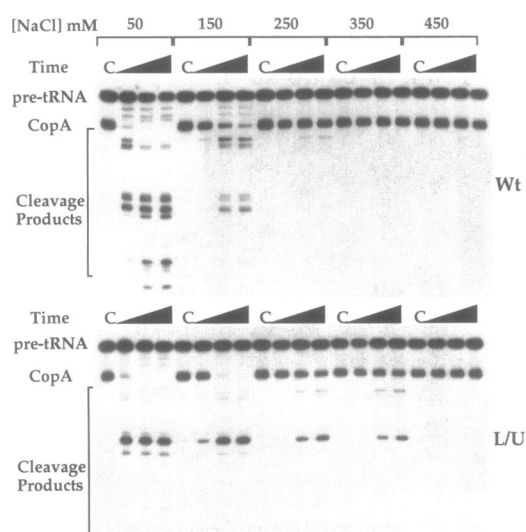


Figure 5. *In vitro* cleavage of CopA-Wt and CopA-L/U RNAs by RNase III as a function of NaCl concentration. Autoradiograms of time courses are shown for a wild-type (upper panel) and an L/U CopA substrate (lower panel). The experimental procedure is given in Materials and Methods. Salt concentrations used are indicated. C denotes controls (no enzyme) and the filled triangles indicate increasing time of incubation (30 s and 6 and 12 min). The positions of pre-tRNA, CopA and CopA cleavage products (brackets) are indicated. Note that the RNase III concentration used in the upper panel (Wt) was 1000 times higher than in the lower panel (L/U).

in vitro assay (150 mM NaCl; Fig. 4). Therefore, we tested cleavage of both the poorest substrate, CopA-Wt, and the best substrate, CopA-L/U, for dependence on salt concentration. Figure 5 shows that as the NaCl concentration is increased, cleavage activity on CopA-Wt is lost, whereas cleavage of CopA-L/U still occurs at 250–350 mM NaCl. Thus, at high salt concentrations that favour specific cleavages, CopA-L/U is a good *in vitro* substrate, whereas CopA-Wt is not. At 450 mM salt, enzyme activity *per se* is decreased, in accord with previous experiments using double-stranded RNA substrates (Wagner,

unpublished; 28). Note that Figure 5 underestimates the superiority of the CopA-L/U substrate, since a 1000-fold higher enzyme concentration was used for CopA-Wt than for CopA-L/U.

The positions of the RNase III cuts in CopA were identified by running samples such as the ones in Figure 4 on a high resolution sequencing gel (Fig. 6). The right-hand panel of Figure 6 shows the major and minor cleavage sites identified. Since high enzyme concentrations were used for CopA-Wt, its cleavage sites may be due to star activity (15,27)

Table 2. Relative specific rates of CopA cleavage by RNase III *in vitro*

CopA substrates	Relative specific cleavage rate \pm SD ^a	
CopA-Wt	1	\pm 14%
CopA-Lo	190	\pm 17%
CopA-Up	20	\pm 24%
CopA-L/U	460	\pm 30%
CopA-Xb	115	\pm 19%

^aSpecific cleavage rates were obtained from the experiment in Figure 4 and two additional duplicate experiments. Relative specific rates were calculated from initial rates of cleavage and multiplied by the dilution factor of a stock solution of RNase III to correct for the different concentrations of enzyme. Specific cleavage rate obtained with the CopA-Wt substrate was set to unity. Average values are given and standard deviations are from the results of three independent experiments.

The steady-state levels of CopA-L/U and CopA-Lo are decreased *in vivo*

Since mutant CopA RNAs were more sensitive to purified RNase III *in vitro* (see Fig. 4), we assayed for steady-state levels of CopA RNA in cells containing plasmids encoding wild-type or mutant CopA (but not target RNA). Total RNA was extracted and Northern analysis performed using a probe specific for CopA (Materials and Methods). For loading standards, the membranes were re-probed with a labelled oligodeoxynucleotide specific for 5S rRNA. Autoradiograms of such an analysis are shown in Figure 7 and the relative steady-state levels of CopA are

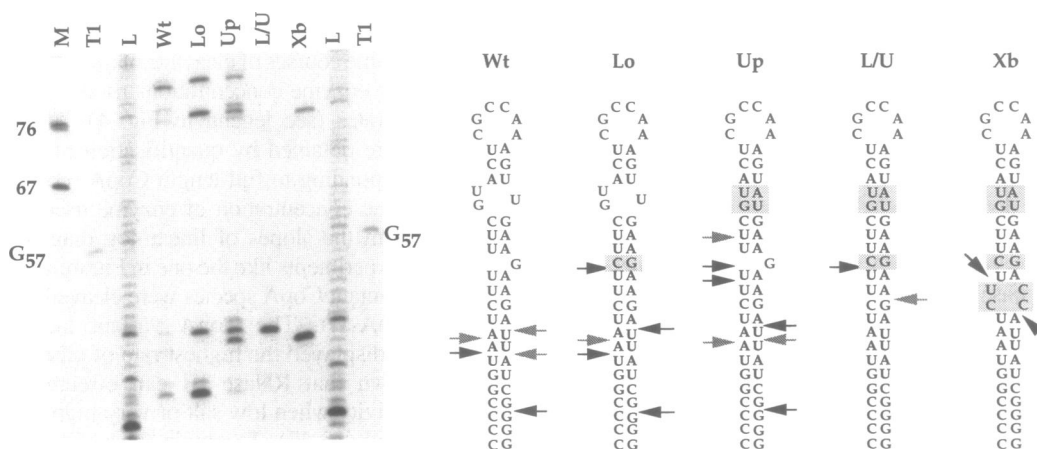


Figure 6. The location of RNase III cleavage sites in mutant and wild-type CopA RNA. Appropriate samples selected from the experiment shown in Figure 4 were electrophoresed next to molecular weight markers (³²P-labelled *Msp*I fragments of pBR322: M), RNase t1 digests of CopA-Wt (T1) and alkaline ladders (L). Some relevant sizes are indicated. The determined positions of cleavage in wild-type and mutant stem-loops II are depicted schematically (major cleavages, solid arrows; minor cleavages; stippled arrows) and can be identified by comparing each band position with the position of G57 and the alkaline ladder.

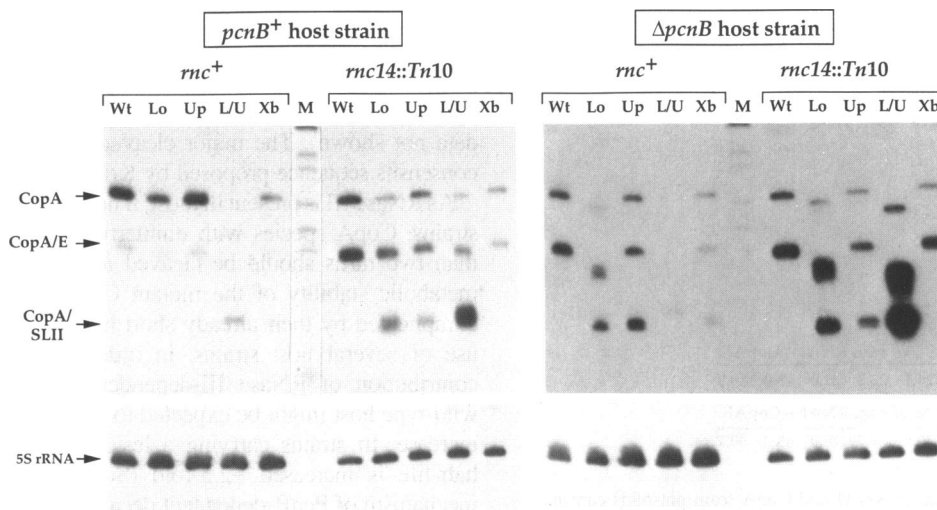


Figure 7. Northern blot analysis of CopA in wild-type and mutant *E. coli* host strains. Total RNA from strains containing plasmids of the pGW58-CA series (encoding *copA*, but deleted for the *repA* promoter) were analysed by Northern blot analysis (Materials and Methods; 18). Filters were first hybridized using an RNA probe complementary to CopA (upper panel). After quantitation of the signal, filters were stripped and subsequently re-probed for ribosomal 5S rRNA (lower panel). The positions of full-length CopA (CopA), an RNase E cleavage product of CopA (CopA/E; 18) and stem-loop II (CopA/SLII; see Results) are indicated. The right-hand gel ($\Delta pcnB$ host strain) was run at somewhat lower temperature, thus resulting in slightly altered gel mobility of mutant RNAs (see Fig. 2). Molecular size markers were ^{32}P -labelled *MspI* fragments of pBR322 (M; sizes from bottom 67, 76, 90, 110, 122, 146 nt; 18). The marker lane of the left-hand panel was taken from a longer exposure of the same film. Calculations of relative CopA steady-state levels are shown in Table 3.

summarized in Table 3. We performed the analysis in four host strains. An RNase III-specific effect on *in vivo* CopA levels should be observable by comparing the patterns obtained in otherwise isogenic *rnc*⁺/*rnc*⁰ strain pairs. Since the normal half-life of CopA is short (~1 min in a wild-type *E. coli* strain in rich medium at 37°C; Söderbom, unpublished), an enhanced decay rate due to the action of RNase III might be expected to contribute little to the overall decay rate. Therefore, we also tested CopA accumulation in $\Delta pcnB$ host strains that either carried the mutated or the wild-type *rnc* allele. In *pcnB* mutant strains, CopA half-life is extended by a factor of 2–3 (Söderbom, unpublished) and the relative contribution of RNase III to overall decay of CopA may be slightly enhanced.

The patterns show bands corresponding to full-length CopA and a CopA species which has been generated by RNase E (CopA/E in Fig. 7; 18; Söderbom, unpublished). In addition, some CopA mutant species of ~55 nt, corresponding to stem-loop II (Fig. 7, CopA/SLII; see also Fig. 1) predominate. This is most striking in an *rnc*⁰ strain background. In *rnc* mutant strains, the steady-state level of CopA-total is increased compared to that in a wild-type host strain (Fig. 7; Table 3). This holds true for both *rnc*⁺/*rnc*⁰ pairs in *pcnB*⁺ and $\Delta pcnB$ backgrounds, even though the *pcnB* mutant strains have lower overall CopA levels due to a decrease in copy number of the vector plasmid (4). The most drastic RNase III-specific effect on degradation is seen with CopA-L/U, where very little CopA is present in *rnc*⁺ strains, but accumulation is evident in *rnc*⁰ backgrounds (Fig. 7; Table 3). A similar, but less pronounced, effect is seen with CopA-Lo. This is most clearly observed in the absence of PcnB, where overall degradation is slowed down. All other changes in band patterns may be attributed to indirect effects of RNase III (see Discussion). In summary, the two mutant CopA species that were most rapidly cleaved by RNase III *in vitro* also showed indications of RNase III-dependent cleavage *in vivo*, whereas the main pathway for degradation of the other CopA species is not primarily dependent on RNase III.

Table 3. Relative steady-state levels of mutant and wild-type CopA RNA in different *E. coli* strains

<i>copA</i> gene on plasmid ^a	Strains used ^(a)			
	<i>rnc</i> ⁺ / <i>pcnB</i> ⁺	<i>rnc</i> ⁰ / <i>pcnB</i> ⁺	<i>rnc</i> ⁺ / <i>pcnB</i> ⁰	<i>rnc</i> ⁰ / <i>pcnB</i> ⁰
<i>copA</i> -Wt	1.00 ^b	1.00 ^b	1.00 ^b	1.00 ^b
<i>copA</i> -Lo	0.59	0.52	0.18	0.96
<i>copA</i> -Up	0.97	0.46	0.56	0.38
<i>copA</i> -L/U	0.07	0.27	0.01	2.76
<i>copA</i> -Xb	0.33	0.23	0.22	0.51

^aThe plasmids and host strains are described in Materials and Methods and Table 1.

^bCalculation was done by dividing the band intensities of all CopA RNA-specific bands by that of 5S rRNA (RNA loading standard) as described in Materials and Methods. For each strain (vertical columns), the ratio of the band intensities CopA-Wt/5S is set to unity.

The bulge mutations do not affect transcription initiation or termination *in vitro*

Measurements of CopA RNA decay after rifampicin treatment is a second way to determine the effect of the mutations. We have performed such experiments, but found the results difficult to interpret, since different degradation pathways are used dependent on the CopA variants tested and on the host strains used (see Discussion). Provided that mutations do not affect initiation and termination of transcription, steady-state levels (Table 3) can be considered a reliable measure of metabolic stability.

Plasmids encoding the various *copA* genes were transcribed *in vitro* in the presence of [γ - ^{32}P]ATP and unlabelled UTP, CTP and GTP. These plasmids also encode RNAI (the replication inhibitor RNA of the ColE1 family of plasmids; 3). Since both RNAI and CopA initiate with ATP, an RNAI-specific signal can serve as a reference for CopA transcription. Thus, this experiment tests transcription initiation activity at the *copA* promoter in competition with the *rnaI* promoter and the band pattern also reveals

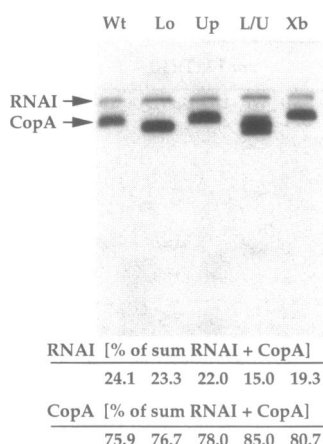


Figure 8. *In vitro* transcription of RNAI and CopA from plasmids carrying mutant or wild-type *copA* genes. Transcription mixtures contained plasmids of the pGW58 series that encode two major ATP-initiated transcripts, RNAI and CopA. Transcription assays in the presence of *E. coli* RNA polymerase and [γ - 32 P]ATP were performed as in Materials and Methods and the labelled products were separated on an 8% sequencing gel. Band intensities were quantified and the relative transcription of RNAI and CopA determined (bottom).

whether termination of transcription is affected. Figure 8 shows that the ratios of the band intensities of the CopA species and RNAI are very similar and that no termination defect is supported.

DISCUSSION

The intracellular concentration of an antisense RNA and its rate constant of binding to the target RNA are the two main factors that determine inhibitory efficiency. In this communication we asked whether the alteration of bulged-out nucleotides in the stem of CopA (the antisense RNA that regulates the copy number of plasmid R1) affects its metabolic stability. The accompanying paper (16) complements this study by reporting the effects of bulged-out nucleotides on target binding and inhibitory activity.

Mutations were introduced into the *copA* gene so that CopA RNAs were generated that lacked one or both of the normal bulges within the upper stem (CopA-Lo, -Up, -L/U; Fig. 1). In addition, one bulge was introduced at a new position (CopA-Xb). Chemical and enzymatic probing confirmed the absence of bulges as predicted from the mutational base changes (Fig. 3). Strikingly aberrant electrophoretic migration of two of the mutant CopA species (CopA-Lo and CopA-L/U; Fig. 2) indicated that removal of the lower, singly bulged G residue results in an altered overall structure.

As restored base pairing within the upper stem region should result in an RNA helix of about two helical turns, mutant CopA species were expected to be substrates for the double-strand-specific RNase III. This was confirmed *in vitro* (Fig. 4; Table 2). Under conditions of specific cleavage, wild-type CopA was protected from RNase III, whereas the mutant CopAs were good substrates. The two superior substrates, CopA-Lo and CopA-L/U, were the same ones that were most affected in overall structure (see above) and carried the longest stretch of uninterrupted helix in stem II. Removal of the upper bulge (CopA-Up; Table 2) enhanced the cleavage rate moderately. The internal loop of CopA-Xb apparently resulted in an RNase III cleavage site reminiscent of structures present in several naturally occurring substrates (15). Accordingly,

the sites of cleavage were staggered on both sides of the new internal loop (Fig. 6). The RNase III cleavage sites were also mapped in each of the other substrates. Cleavage occurred in the helical region of stem II, but not in the 5'-half of CopA (Fig. 6 and data not shown). The major cleavage sites do not resemble the consensus sequence proposed by Krinke and Wulff (29).

As RNase III is present in most, if not all, bacterial wild-type host strains, CopA species with uninterrupted RNA helices of more than two turns should be cleaved *in vivo* as well. The test for metabolic stability of the mutant CopA species was, however, complicated by their already short half-lives. This suggested the use of several host strains, in order to be able to assess the contribution of RNase III-dependent degradation, which in a wild-type host might be expected to yield only a small decay rate increase. In strains carrying a lesion in the *pcnB* gene, CopA half-life is increased ~2.5-fold (Söderbom, unpublished). The mechanism of PcnB-dependent decay is not understood (4,5), but the analysis of degradation intermediates suggests that 3'-end-initiated decay may be slowed down (Söderbom, unpublished). From the quantitative and qualitative analysis of relative steady-state levels of CopA (in *mrc*⁺/*mrc*⁰ strain pairs carrying either the wild-type or the mutant *pcnB* allele), some clear results were obtained. The intracellular concentration of CopA-L/U and, to a lesser degree, CopA-Lo was decreased in RNase III-proficient strains (Fig. 7; Table 3). As expected, the RNase III-dependence of this effect was more pronounced when (presumed) RNase III-independent decay was slowed down by the effect of the *pcnB* mutation. CopA-Up and CopA-Xb showed no clear indications of RNase III-specific decay. CopA-Up was the most slowly cleaved mutant RNA *in vitro* (Fig. 4; Table 2). In contrast, CopA-Xb was cleaved well *in vitro*, but failed to show clear *mrc*-dependent steady-state changes *in vivo*. We cannot as yet explain this result.

Figure 7 also indicated an additional effect of the bulge mutations. Bands corresponding to CopA RNAs of ~55 nt in length accumulated. These RNAs correspond to stem-loop II (data not shown) and are most dominant in an *mrc*⁰ background. Their abundance decreased in the order CopA-L/U, CopA-Lo, CopA-Up, whereas these species were essentially absent in the lanes representing CopA-Wt and CopA-Xb. This is consistent with the order of the predicted thermodynamic stabilities (30) of the five different 3'-terminal stem-loops, which follows the order of abundance of the stem-loop II-specific band intensities obtained in the *mrc* mutant strains. Since the presence of RNase III prevents the accumulation of these RNAs, we suggest that the presence of extended helical structure on the one hand will create RNA substrates for RNase III cleavage, but on the other hand may impede exonucleolytic degradation. The latter interpretation is supported by recent studies of RNA-OUT decay (14), where 3' exonuclease-dependent antisense RNA decay was determined as a function of predicted ΔG^0 of RNA-OUT mutants. Thus, the presence of bulges in CopA results in a structural destabilization that may favour exonuclease-dependent decay, but plays a protective role against RNase III.

A common problem with the analysis of *mrc*-dependent phenotypes *in vivo* is that of pleiotropic effects. Thus, in the absence of RNase III the expression of many genes is altered (15). In particular, the level of PNPase is raised in *mrc* strains (31), which is expected to cause changes in RNA stability. Therefore, we cannot draw conclusions about the steps in the degradation pathway of CopA RNAs beyond those indicated above.

The results presented above do not tell us why bulges/internal loops interfere with RNase III activity. The structural requirements of the enzyme are not yet well defined. Clearly, completely double-stranded RNAs are cleaved, but most natural processing sites carry internal loops that do not abolish activity (15). A double-stranded RNA mimicry model has been suggested in which an internal loop can engage in tertiary interactions that mimic an authentic double-stranded RNA helix (32), but this model was refuted by a mutational analysis (33). Similarly, the role of a short CUU/GAA 'consensus' sequence near the cleavage site, proposed to be involved in substrate selection and cleavage activity, has been called into question (33).

Thus, the reason why the bulges in CopA protect this RNA from RNase III-mediated cleavage is not understood. In the *rpsO-pnp*, *rnc*, *metY-orf15A-nusA* and λ *sib* transcripts, RNase III cleavage sites are located in double-stranded regions (15). In phage T7 early RNAs, processing of sites close to 1.2 (R5) and 0.3 respectively were identified within internal loops or bulges. Mutational changes that destabilized double helices in the T7 R5 stem region or in that of λ *sib* RNA respectively prevented RNase III cleavage (see references in 15). Also, Chelladurai *et al.* (27) have shown that a mutated RNA substrate in which an internal loop has become fully base paired has strongly increased binding affinity for RNase III. This may suggest that the higher cleavage activity of the fully base paired CopA-L/U (and to a lesser extent CopA-Lo) is in part due to a decrease in K_m . Since this communication is primarily concerned with the role of bulges in affecting the metabolic stability of CopA, we have not attempted to analyze the relative contributions of the mutations to changes in k_{cat} and K_m respectively.

Bulged-out nucleotides certainly play roles in addition to the one discussed in this communication. In many cases, these substructures serve as (part of) protein recognition sites on RNAs (see, for example, 34). As we show in the accompanying paper, the presence of the bulges in CopA is required for rapid duplex formation with CopT *in vitro*, as well as for effective inhibition of target RNA function *in vivo*. Thus, in the CopA/CopT system, the protective role of bulges is evident, but quantitatively of minor importance to antisense RNA control (16). With respect to the results shown here, which seem to indicate that most changes within this naturally occurring antisense RNA system decrease its biological effectiveness, it is difficult to specify suggestions for the design of artificial antisense RNAs. However, we suggest that considerations of structural elements in the RNAs is of importance, both with respect to their contribution to the metabolic stability in the specific cell type of choice and to their effect on binding rates to the selected target.

ACKNOWLEDGEMENTS

We thank S. Andersson for expert technical assistance, L. Kirsebom for synthesis of oligodeoxyribonucleotides and D. Court for providing purified RNase III. We are grateful to K. Nordström and D. Andersson for critical reading of the manuscript. This work was supported by The Swedish Natural Science Research Council and the Swedish Board for Technical Development.

REFERENCES

- 1 Wagner, E.G.H. and Simons, R. (1994) *Annu. Rev. Microbiol.* **48**, 713–742.
- 2 Persson, C., Wagner, E.G.H. and Nordström, K. (1988) *EMBO J.* **7**, 3279–3288.
- 3 Tomizawa, J. (1984) *Cell* **38**, 861–870.
- 4 He, L., Söderbom, F., Wagner, E.G.H., Binnie, U., Binns, N. and Masters, M. (1993) *Mol. Microbiol.* **9**, 1131–1142.
- 5 Xu, F., Lin-Chao, S. and Cohen, S.N. (1993) *Proc. Natl. Acad. Sci. USA* **90**, 6756–6760.
- 6 Nordström, K., Molin, S. and Light, J. (1984) *Plasmid* **12**, 71–90.
- 7 Nordström, K. and Wagner, E.G.H. (1994) *Trends Biochem. Sci.* **19**, 294–300.
- 8 Blomberg, P., Nordström, K. and Wagner, E.G.H. (1992) *EMBO J.* **11**, 2675–2683.
- 9 Blomberg, P., Engdahl, H.M., Malmgren, C., Romby, P. and Wagner, E.G.H. (1994) *Mol. Microbiol.* **12**, 49–60.
- 10 Lacatena, R.M. and Cesarini, G. (1983) *J. Mol. Biol.* **170**, 635–650.
- 11 Kittle, J.D., Simons, R.W., Lee, J. and Kleckner, N. (1989) *J. Mol. Biol.* **210**, 561–572.
- 12 Hjalt, T. and Wagner, E.G.H. (1992) *Nucleic Acids Res.* **20**, 6723–6732.
- 13 Persson, C., Wagner, E.G.H. and Nordström, K. (1990) *EMBO J.* **9**, 3767–3775.
- 14 Pepe, C.M., Maslesa-Balic, S. and Simons, R.W. (1994) *Mol. Microbiol.* **13**, 1133–1142.
- 15 Court, D. (1993) in *Control of Messenger RNA stability* (Eds Belasco, J.G. and Brawerman, G.), Academic Press, pp. 71–116.
- 16 Hjalt, T.H. and Wagner, E.G.H. (1995) *Nucleic Acids Res.* **23**, 580–587.
- 17 Masters, M., Colloms, M.D., Oliver, I.R., He, L., Macnaughton, E.J. and Charters, Y. (1993) *J. Bacteriol.* **175**, 4405–4413.
- 18 Blomberg, P., Wagner, E.G.H. and Nordström, K. (1990) *EMBO J.* **9**, 2331–2340.
- 19 Taylor, J.W., Schmidt, W., Cosstick, R., Okruszek, A. and Eckstein, F. (1985) *Nucleic Acids Res.* **13**, 8749–8764.
- 20 Taylor, J.W., Ott, J. and Eckstein, F. (1985) *Nucleic Acids Res.* **13**, 8765–8785.
- 21 Bertani, G. (1951) *J. Bacteriol.* **62**, 293–300.
- 22 Sambrook, J., Fritsch, E.F. and Maniatis, T. (1989) *Molecular Cloning: A Laboratory Manual*. Cold Spring Harbor Laboratory Press, Cold Spring Harbor, NY.
- 23 Wagner, E.G.H. and Nordström, K. (1986) *Nucleic Acids Res.* **14**, 2523–2538.
- 24 Gornicki, P., Baudin, F., Romby, P., Wiewiorowski, M., Kryzosiak, W., Ebel, J.P., Ehresmann, C. and Ehresmann, B. (1989) *J. Biomol. Struct. Dyn.* **6**, 971–983.
- 25 Hardt, W.-D., Schlegel, J., Erdmann, V.A. and Hartmann, R.K. (1993) *Biochemistry* **92**, 13046–13053.
- 26 Ehresmann, C., Baudin, F., Mougel, M., Romby, P., Ebel, J.P. and Ehresmann, B. (1987) *Nucleic Acids Res.* **22**, 9109–9128.
- 27 Chelladurai, B., Li, H., Zhang, K. and Nicholson, A.W. (1993) *Biochemistry* **32**, 7549–7558.
- 28 Li, H.-L., Chelladurai, B.S., Zhang, K. and Nicholson, A.W. (1993) *Nucleic Acids Res.* **21**, 1919–1925.
- 29 Krinke, L. and Wulff, D.L. (1990) *Nucleic Acids Res.* **18**, 4809–4815.
- 30 Freier, S.M., Kierzek, R., Jaeger, J.A., Sugimoto, N., Caruthers, M.H., Neilson, T., Turner, D.H. (1986) *Proc. Natl. Acad. Sci. USA* **83**, 9373–9377.
- 31 Portier, C., Dondon, L., Grunberg-Manago, M. and Régnier, P. (1987) *EMBO J.* **6**, 2165–2170.
- 32 Robertson, H.D. and Barany, F. (1978) in *Proceedings of the 12th FEBS Congress*, Pergamon Press, NY, pp. 285–295.
- 33 Chelladurai, B.S., Li, H. and Nicholson, A.W. (1991) *Nucleic Acids Res.* **19**, 1759–1766.
- 34 Peattie, D.A., Douthwaite, S., Garrett, R.A. and Noller, H.F. (1981) *Proc. Natl. Acad. Sci. USA* **78**, 7331–7335.
- 35 Casadaban, M.J. and Cohen, S.N. (1980) *J. Mol. Biol.* **138**, 179–207.
- 36 Gough, J. and Murray, N. (1983) *J. Mol. Biol.* **166**, 1–19.
- 37 Plumberidge, J.A., Dondon, J. and Nakamura, Y. (1985) *Nucleic Acids Res.* **13**, 3371–3388.
- 38 Ryder, T. B., Davison, D.B., Rosen, J.I., Ohtsubo, E. and Ohtsubo, H. (1982) *Gene* **17**, 299–310.